

RSC Advances



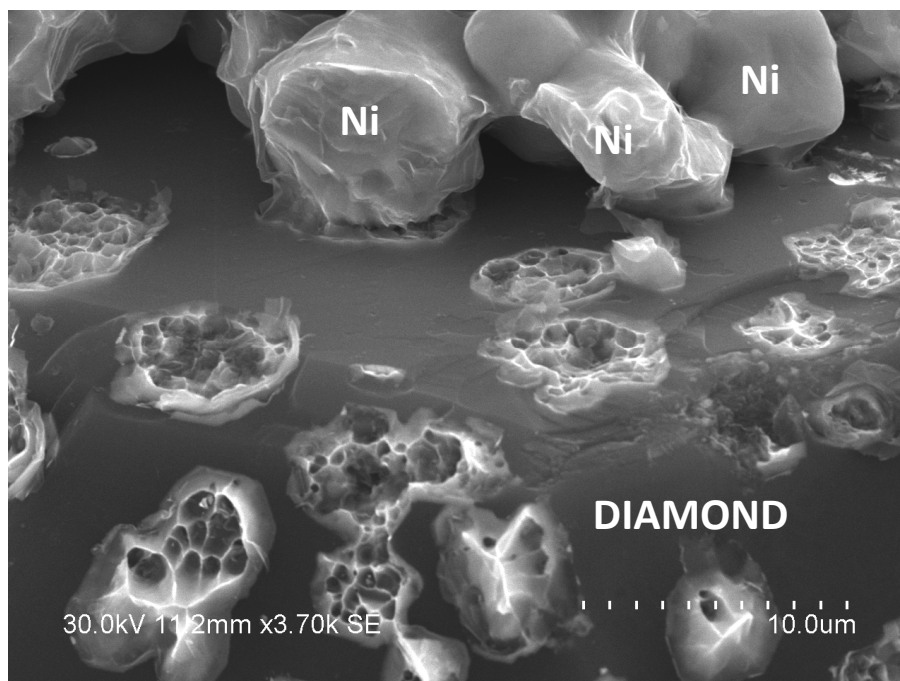
This is an *Accepted Manuscript*, which has been through the Royal Society of Chemistry peer review process and has been accepted for publication.

Accepted Manuscripts are published online shortly after acceptance, before technical editing, formatting and proof reading. Using this free service, authors can make their results available to the community, in citable form, before we publish the edited article. This *Accepted Manuscript* will be replaced by the edited, formatted and paginated article as soon as this is available.

You can find more information about *Accepted Manuscripts* in the [Information for Authors](#).

Please note that technical editing may introduce minor changes to the text and/or graphics, which may alter content. The journal's standard [Terms & Conditions](#) and the [Ethical guidelines](#) still apply. In no event shall the Royal Society of Chemistry be held responsible for any errors or omissions in this *Accepted Manuscript* or any consequences arising from the use of any information it contains.

Microstructural investigations of the material adjacent to the nickel/diamond interface formed during low temperature sintering allow suggesting contact melting of a metastable eutectic as a process responsible for the interface formation and development in this system.





Journal Name

ARTICLE

Towards a better understanding of nickel/diamond interactions: the interface formation at low temperatures

B. B. Bokhonov,^{a, b} A. V. Ukhina,^a D. V. Dudina,^{b, c} K. B. Gerasimov,^a A. G. Anisimov,^c V. I. Mali^cReceived 00th January 20xx,
Accepted 00th January 20xx

DOI: 10.1039/x0xx00000x

www.rsc.org/

We report the formation and development of the interface between diamond and nickel in partially densified compacts obtained from powder mixtures by Spark Plasma Sintering, hot pressing and conventional sintering at 700 and 900 °C — temperatures, which are well below the melting point of nickel and even below the nickel-graphite eutectic. The nickel particles sintered between themselves and formed joints with facets of the diamond crystals. Most of these joints fractured cohesively leaving Ni-containing patches on the diamond facets. The microstructure of the patches adhered to the diamond surface in compacts sintered at 900 °C, their geometry and orientation relative to the edges of the diamond facets suggest that the formation and development of the nickel/diamond interface are associated with melting and solidification of the melt according to certain directions of the diamond crystalline lattice. A possible explanation of the formation of liquid at such a low temperature is contact melting of a metastable eutectic between nickel and diamond.

Introduction

The interaction at the nickel/diamond interface is a key question in a variety of applications, such as epitaxial growth of diamond films on nickel substrates [1-2], catalytic etching of diamond surfaces [3-8], and design of diamond-metal composites with nickel-containing binders [9-11]. It is also of great interest from the fundamental point of view as the processes occurring at the nickel/diamond interface exemplify the interaction between two phases, one of which is metastable. An appreciable solubility of carbon in nickel [12] makes the latter, on the one hand, a suitable catalyst for diamond growth at high pressures. On the other hand, at low pressures, nickel catalyzes graphitization of diamond. According to the equilibrium nickel-graphite phase diagram at 1 atm [12], a eutectic exists between nickel and graphite at 1326 °C; however, little is known on the existence of a nickel-diamond eutectic. A possibility of melting at the diamond/nickel interface has been a matter of discussion [1-2, 8]. Smirnov et al. [8] observed the formation of self-organized nanoparticles of nickel from a thin film on the diamond surface at 1000 °C in a flow of hydrogen. They suggested that melting was involved in that process and thus must have occurred at a

temperature much lower than the melting point of nickel or the nickel-graphite eutectic. This agreed with observations of Yang et al. [1-2], who obtained evidence of the presence of molten phases surrounding diamond nuclei during the formation of diamond films on nickel substrates and argued that hydrogen diffusion into the metal plays an important role in lowering its melting temperature. However, the exact onset temperature of interaction between diamond and nickel brought into contact at low pressures in a hydrogen-free environment has not been determined.

In this work, we observed the formation and analyzed the development of the nickel/diamond interface in compacts partially densified by Spark Plasma Sintering (SPS), hot pressing and conventional sintering of powder mixtures. Multiple capabilities and advantages of the SPS as a consolidation method are visible from the recent literature. SPS enables efficient consolidation [13-14], preservation of uniform grain size [15], formation of mechanically robust partially densified (porous) structures [16], flexibility of microstructure reorganization [17] and design [18] as well as in situ synthesis of compounds from powder reactants having a large difference in their melting points or vapour pressures [19]. For metal-diamond materials, SPS has the potential of establishing strong inter-particle bonding while preventing undesirable metal-catalyzed graphitization at the interface.

As the processes at inter-particle contacts are crucial for the outcome of consolidation, they were addressed in a number of studies [20-23]. The evolution of the morphology and microstructure of inter-particle necks forming between particles of the same material was discussed as directly related to the effects of electric current passing through the contacts and electrical discharges in the case of contacts that are poorly established. Studies of sintering between particles of different

^aInstitute of Solid State Chemistry and Mechanochemistry SB RAS, Kutateladze str. 18, Novosibirsk, 630128, Russia.

^bNovosibirsk State University, Pirogova str. 2, Novosibirsk, 630090, Russia.

^cLavrentyev Institute of Hydrodynamics SB RAS, Lavrentyev ave. 15, Novosibirsk, Russia.

† Corresponding author: Prof. Boris B. Bokhonov, Dr. Sci., Institute of Solid State Chemistry and Mechanochemistry SB RAS, Kutateladze str. 18, Novosibirsk 630128, Russia, tel. 7-383-233-24-10, fax 7-383-332-28-47, E-mail: bokhonov@solid.nsc.ru

Electronic Supplementary Information (ESI) available: See DOI: 10.1039/x0xx00000x

materials are much more challenging, as they involve the formation of new interfaces and possibly new phases as a result of chemical interactions. A significant step in this direction was made by Rudinsky & Brochu [24], who investigated interdiffusion between particles of nickel and copper — metals with unlimited mutual solubility — during the SPS. However, until now, no study has focused on the microstructure evolution associated with the formation and development of interfaces within contact regions between particles of dissimilar materials. Although electric current does not pass through the nickel/diamond interface, the application of uniaxial pressure through the SPS cycle will induce plastic deformation and yielding of the metal binder with increasing temperature, promoting the formation of new contacts of the metal with the diamond grains. Furthermore, electric current-induced localized heating and melting of contacts between nickel particles that also touch diamond facets can contribute to an increase in the interfacial area in the system. In order to get further insights into the processes at the nickel/diamond interface, we conducted comparative microstructural studies on Spark Plasma Sintered, hot pressed and conventionally sintered nickel-diamond compacts at 700 and 900 °C — temperatures well below the melting point of the nickel-graphite eutectic.

Materials and Methods

Synthetic diamond powder (particle size 70-100 µm) and carbonyl nickel (99.9% purity, <20 µm) were used to prepare the mixtures for consolidation. The diamond particles are crystals of cuboctahedron shape (Fig.1S (a-b)). As can be seen from Fig.1S (c) the micron-sized nickel particles having nearly spherical shape are not agglomerated; however, each particle has a rather rough surface showing grains less than 1 µm in size. SPS and hot pressing experiments were conducted using a 50 vol.% nickel – 50 vol.% diamond mixture. For conventional sintering, a 80 vol.% nickel – 20 vol.% diamond mixture was used to make cold pressing of the pellet easier. A comparative conventional sintering experiment was performed with a mixture containing the same volume content of iron instead of nickel. Carbonyl iron powder (particle size 5 µm, 99.9%) was used.

SPS of the powders was carried out using a SPS Labox 1575 apparatus (SINTER LAND Inc.). A graphite die of 10 mm inner diameter and 50 mm outer diameter and tungsten punches of 10 mm diameter were used. The die wall was lined with carbon foil. The circles of tantalum foil were placed between the flat ends of the punches and the sample. In this configuration, the electric current was passing through all elements of the assembly: the punches, the die, and the sample (Fig.2S). The temperature during the SPS was controlled by a pyrometer focused on a cylindrical hole 2 mm in diameter and 8 mm deep in the wall of the die at its mid-plane. The die was wrapped in a piece of graphite felt in order to reduce the radiation heat losses and corresponding temperature gradients between the wall of the die and the sample. Model experiments on sintering of copper-containing

materials conducted with the same die/punch/sample configuration and temperature measurement method and using massive melting of the metal as a temperature marker showed that the temperature of the sample is higher than the pyrometer-measured temperature, and this difference is approximately 100 °C. SPS was conducted in vacuum. An average heating rate of 50 °C·min⁻¹ was used. The sample was held at the maximum temperature of 900 °C for 5 min and then cooled down to room temperature. At the beginning of the sintering cycle, a uniaxial pressure of 40 MPa was applied and kept constant through the sintering cycle. Hot pressing was conducted in argon at 700 °C for 5 min at a uniaxial pressure of 40 MPa using a graphite die with 12 mm inner diameter and graphite punches. Conventional sintering of a cold-pressed compact of 10 mm diameter was conducted in a vacuum furnace at 900 °C for 1 h. The sintering temperatures selected in this study were much lower than the nickel-graphite eutectic temperature, as is marked on the nickel-graphite phase diagram in Fig.3S. The partially sintered nickel-diamond specimens were 2-3 mm thick. The relative density of the sintered compacts was calculated using the specimen weight and dimensions (measured after the protective foil has been removed) and the theoretical density of the selected composition. The relative density of the sintered compacts was 75-80%.

The phase composition of the sintered compacts was studied by X-ray diffraction (XRD) using Cu K α radiation. The XRD patterns were recorded using a D8 ADVANCE diffractometer (Bruker AXS). The microstructural studies were carried out using a Hitachi-3400S Scanning Electron Microscope working at 30 kV and equipped with an Energy-Dispersive Spectroscopy unit (NORAN Spectral System 7, Thermo Fisher Scientific Inc.). The elemental maps were obtained using 10 scans of a selected area of the sample. The elemental analysis was conducted in an automatic mode, no standard samples were used. Fracture surfaces of the compacts were studied. Colour images were created corresponding to the results of the elemental mapping of the areas. Differential Scanning Calorimetry (DSC) and thermogravimetric (TG) analyses were performed using a STA 449 F/1/1 JUPITER thermal analysis instrument (Netzsch) in a flow of argon (up to 1500 °C) and hydrogen (up to 1300 °C) at a heating rate of 20 K·min⁻¹. For the experiment in hydrogen, the mass-spectrum was collected using a QMS403 CF AEOLUS mass-spectrometer.

Results and Discussion

As can be concluded from the XRD pattern of the sintered compact, SPS consolidation of the nickel-diamond mixture proceeded without any noticeable phase changes (Fig.1 (a)). The size ratio of nickel and diamond particles in the mixture and the volume ratio of the phases were such that in the compact, the diamond crystals were embedded in a partially sintered nickel matrix (Fig.1 (b)). Nickel particles sintered between themselves forming necks while their fine-structured surface observed in the starting powder became smoother.

During SPS, heating under pressure led to sintering between the nickel particles and the facets of the diamond crystals (Fig.1 (c)). The facets of the diamond crystals observed on the fracture surface of the Spark Plasma Sintered compact were covered with patches 5-10 μm in size (Fig.2 (a)) distributed quite uniformly. The patches showed a dimpled morphology characteristic of ductile fracture (Fig.4S). The same morphology was observed on the fracture surface of the partially sintered nickel binder (Fig.2 (e)). The colour image of the patches on the diamond facets corresponding to the elemental maps of carbon and nickel indicate that they contain

nickel (Fig.2 (b-d), Fig.5S). This indicates that the fracture of the nickel-diamond inter-particle joints was cohesive while strong bonding was established at the nickel/diamond interface. An indication of the interaction-caused material redistribution is the presence of carbon on the surface of the other halves of the fractured joints (fracture surface of the nickel particles that had been in contact with the diamond crystals). The presence of carbon in such locations (Fig.2 (f-g)) points to the dissolution of carbon in nickel at the interface and involvement of a certain volume of a nickel particle in the formation of a joint with a diamond facet.

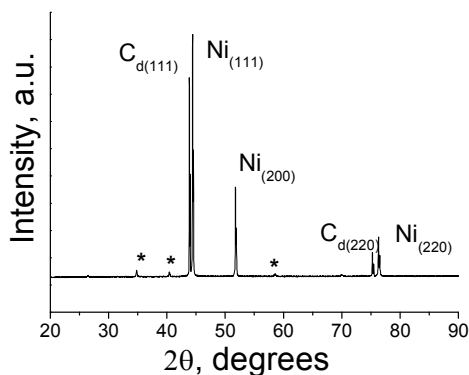
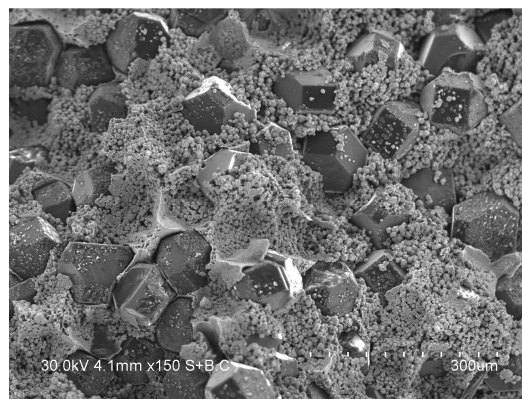
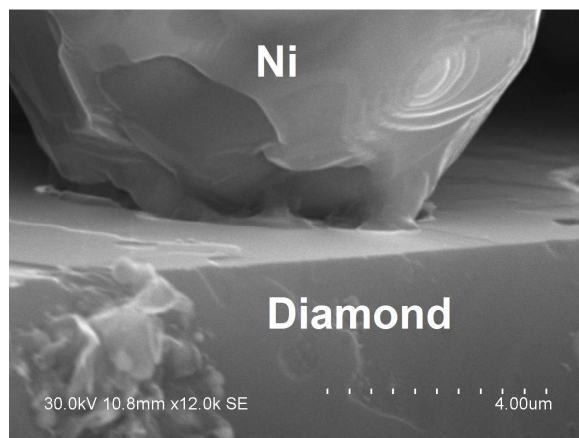
**a****b****c**

Figure 1. XRD pattern of the nickel-diamond compact Spark Plasma Sintered at 900 °C (a), peaks marked with '*' are due to the presence of small amounts of tantalum carbide TaC formed as a results of interaction of the surface of the compact with the tantalum protecting foil; a general view of the fracture surface of the nickel-diamond compact Spark Plasma Sintered at 900 °C (b); the joint between a nickel particle and a diamond facet (c).

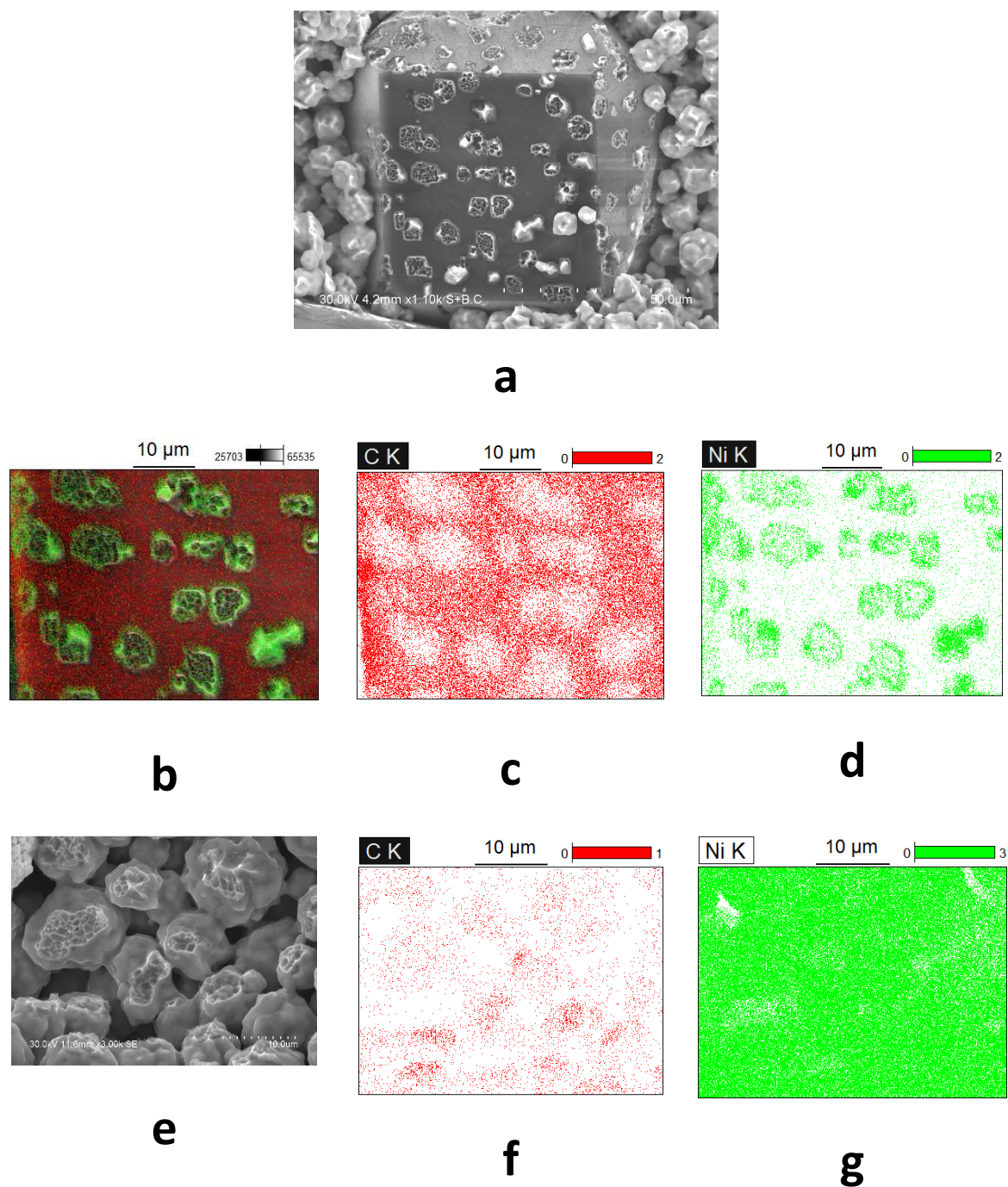


Figure 2. Fracture surface of the nickel-diamond compact Spark Plasma Sintered at 900 °C showing a (100) facet of a diamond particle with patches — a result of cohesive fracture of the nickel-diamond joints (a); colour image of an area of a (100) diamond facet (b); elemental maps of carbon (c) and nickel (d) corresponding to (b); fracture surface of the nickel binder (e); elemental maps of carbon (f) and nickel (g) corresponding to (e).

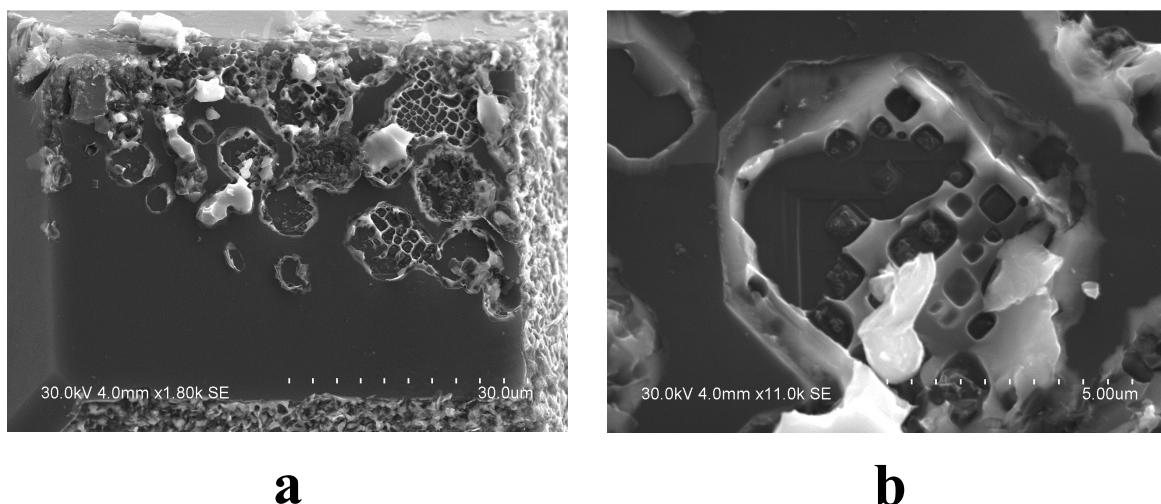


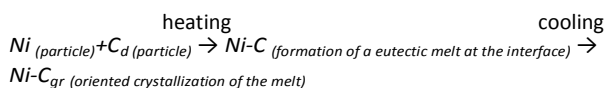
Figure 3. Patches on a (100) facet of a diamond particle observed on the fracture surface of the nickel-diamond compact conventionally sintered at 900 °C (a); microstructural details of a nickel particle adhered to a diamond facet and transformed as a result of the interaction at the diamond/nickel interface (b).

An interesting observation is the formation of patches with shape close to square and boundaries parallel to the edges of the {100} facets and corresponding to $\langle 110 \rangle$ directions. The crystallographic relationships at the interface between nickel and diamond are well known: the epitaxial growth of diamond on nickel [1-2] and nickel on diamond [25-26] with {100} planes of diamond parallel to {100} planes of nickel is possible owing to close values of nickel and diamond lattice parameters. The presence of crystallographic relationships between the Ni-containing patches and the diamond facets in the sintered compact implies that no graphite layer formed at the interface between diamond and nickel. In order to answer the question, whether or not the crystallographic orientation of the patches and the microstructural features of the volume of a nickel particle involved in the formation of a joint are characteristic of the SPS processing, hot pressing and conventional sintering of the nickel-diamond mixtures were also conducted. The differences between the outcomes of these three consolidation procedures were mainly caused by the presence or absence of pressure during heating. Neither conventionally sintered nor hot pressed compacts contained graphite in amounts detectable by the XRD (Fig.6S). The microstructural studies of the nickel-diamond compact hot pressed at 700 °C showed that even at such a low temperature the nickel/diamond interface is established by sintering of nickel particles to diamond facets (Fig.7S), although the patches remaining of the diamond facets are smaller in size. After cooling and fracturing the conventionally sintered nickel-diamond compact, we found areas of nickel-diamond interaction of similar microstructures. However, these areas were rather non-uniformly distributed, sometimes covering the whole facet of a diamond crystal (Fig.3, Fig.8S (a-b)) in contrast with the SPS-processed compact, in which numerous joints with smaller cross-sections formed. This difference is seemingly due to the application of pressure through the

sintering cycle and plastic deformation and yielding of the nickel matrix at the upper temperatures of the heating range. Indeed, the formation of an intimate contact of a certain area at the metal/carbon interface is critical for the metal-assisted transformation of carbon. Our previous experiments on annealing of the nickel-soot powder mixtures (without pre-consolidation) at 900 °C did not reveal any graphite due to a lack of intimate contact between nickel and amorphous carbon particles. However, when a well-developed interface was established by preliminary mechanical milling [27] or by applying pressure during SPS, graphitization in the nickel-amorphous carbon mixtures occurred easily [28].

Some microstructural details of the fracture surface of conventionally sintered compacts are worth particular attention as they shed light on the nature of interactions at the nickel/diamond interface. Apart from the patches on the facets of diamond particles corresponding to cohesive fracture of the nickel-diamond inter-particle joints (Fig.8S (c)), those formed as a result of nickel particles' adhering to the diamond facets were also observed (Fig.3 (b), Fig.9S). The resultant microstructure of such adhered particles is very interesting: it shows cells with walls of specific orientation relative to the edges of the diamond facets. So, the patches of both types have structural elements that are in an orientation relationship with diamond. The volume of the material experiencing transformations associated with the formation of the nickel/diamond interface is large enough to suggest that the most likely scenario of the development of the nickel/diamond interface involves melting and crystallization of the melt along certain directions of the diamond lattice. To start with, it is possible to consider the formation of a liquid phase due to melting of fine nickel grains contained in the initial polycrystalline powder particles (Fig.1S (c)). In this case, a reduction of several hundred degrees in the melting temperature has to be assumed. Another possibility that can

be suggested is the formation of a molten phase due to the existence of a metastable eutectic between nickel and diamond, which appears to be far more likely than the assumption of the lowering of the melting temperature of nickel due to the particle size effect. From the geometry and orientation of the nickel patches, it can be concluded that crystallization of the melt upon cooling follows selected crystallographic directions of the diamond lattice. Therefore, we suggest the following scheme to describe the formation and development of the nickel-diamond interface:



where C_d and C_{gr} designate diamond and graphite, respectively.

The crystallization of the melt creates conditions favourable for the formation of the interface according to the epitaxial relationship between nickel and diamond. For comparison, we conducted the same conventional sintering experiment with iron, which cannot form epitaxial structures with diamond. The fact that no crystallographic relationships between iron patches (found occasionally) and the edges of the diamond facets (Fig.10S-11S) were detected shows that similarities between crystalline lattices of diamond and metal are crucial for the development of crystallographic and microstructural features of the metal/diamond interface and volumes of the material adjacent to it. Upon crystallization of the melt, carbon precipitates as graphite. In order to find out

how the nickel-diamond system behaves upon further heating, a DSC run on the Spark Plasma Sintered nickel-diamond compact was conducted up to 1500 °C in argon. It allowed us to observe an endothermic peak corresponding to melting of the nickel-graphite eutectic at 1329 °C, which agrees well with the existing nickel-graphite equilibrium phase diagram [12]. No melting of pure nickel was detected, which shows that upon heating up to the temperature of the equilibrium eutectic, nickel become saturated with carbon dissolving from the surface of diamond particles. The shape of the diamond crystals was basically preserved in the material after the DSC run and the evidence of solidification of the melt was found in the microstructure.

The atmosphere, in which sintering or annealing of metal-diamond materials is conducted, plays a decisive role in the formation and evolution of the interfaces [29]. In the presence of hydrogen, metallic particles placed in contact with diamond catalyze etching of the surface through the removal of carbon atoms and the concomitant formation of CH_x species, particularly CH_4 [6]. When a piece of the Spark Plasma Sintered nickel-diamond compact was heated up to 1300 °C in a flow of hydrogen in a DSC experiment, etch pits formed on the diamond facets (Fig.4 (a), Fig.12S, Fig.13S (a-d)). Heating the compact in the presence of hydrogen completely altered the structure of the nickel-diamond interface formed during SPS (Fig.4 (b)).

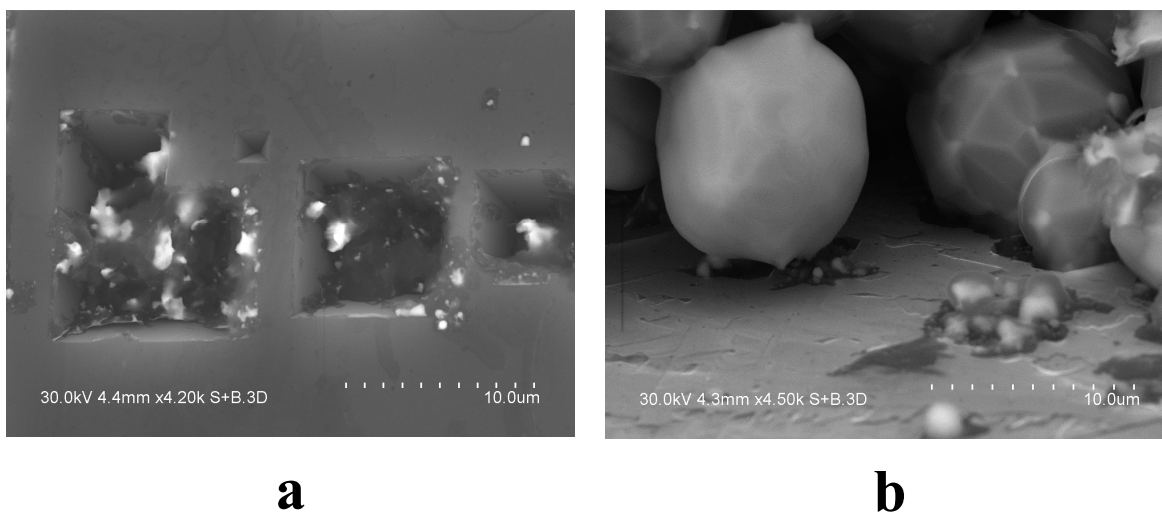


Figure 4. Etch pits formed on the surface of the diamond particles after a DSC run in hydrogen on the nickel-diamond compact Spark Plasma Sintered at 900 °C (a); contact between a nickel particle and the surface of a diamond particle in the Spark Plasma Sintered nickel-diamond compact after a DSC run in hydrogen (b).

The weight losses evident from the TG curve (Fig.5 (a)) were due to evolution of methane CH_4 , as was confirmed by the mass spectrum of the gaseous products (Fig.5 (b)). Etching of the diamond proceeded through the removal of carbon atoms

from the areas contacting with the crystallized (metastable) eutectic in the Spark Plasma Sintered compact. The result of etching was the formation of pits having well-defined orientations of the walls. A small amount of graphite (about 5

wt.%, as estimated from the XRD profile) formed in this process (Fig.14S). This is not surprising, as nickel can induce graphitization at elevated temperatures in parallel to hydrogen-enabled etching. After heating in hydrogen, the character of fracture of the joints had changed: it was no longer cohesive, with nickel particles almost fully separated

from the etched regions. Only fine nickel particles (less than 1 μm in size) were still present near the edges of the etch pits (Fig.13S (b)). Similarly to the sintered compacts, nickel particles forming the joint maintained a certain concentration of carbon dissolved into the nickel from diamond (Fig.13S (e-g)).

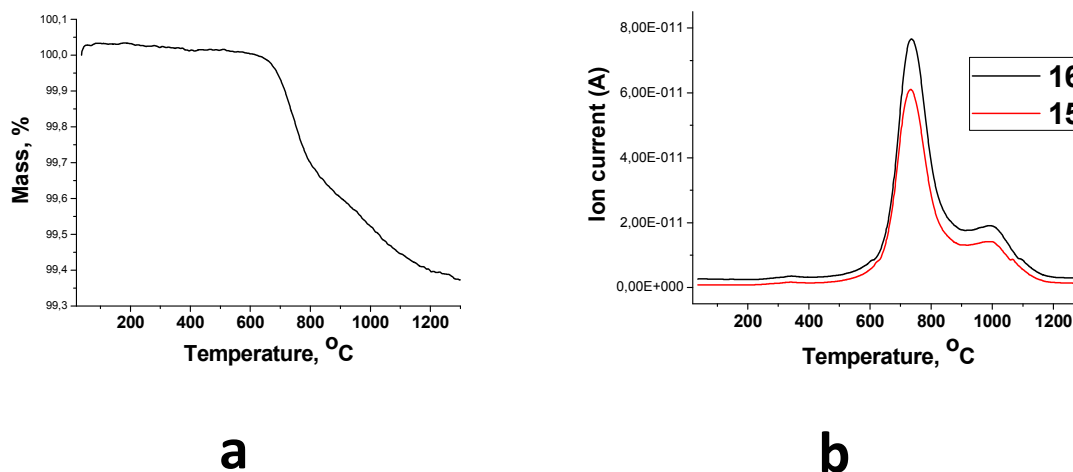


Figure 5. TG curve (a) and mass-spectrum recorded during heating of the Spark Plasma Sintered nickel-diamond compact in a flow of hydrogen (b).

Although the preparation procedures of nickel-diamond composites have been described in many publications (see, for example, [9-10]), the description of the phase changes at the interface during consolidation of powder mixtures at elevated temperatures did not extend beyond graphitization of the subsurface layers of diamond grains. Discharge sintering of nickel-diamond composites in microwave plasma of pre-pressed compacts at 1000 °C was attempted by Twomey et al. [11] with results of faster sintering compared with furnace sintering, however, the structure of the nickel/diamond interface was not given special consideration. As far as mechanical characteristics of the interface are concerned, a patent given in ref. [30] is worth mentioning. It reports the formation of a joint of a high bond strength (258 MPa) between a nickel rod and a diamond plate brought in contact and annealed at 800 °C. Thermal erosion of the diamond surface by nickel was investigated by Tanaka et al. [31]. In their experiments, diamond surfaces were brought into contact with powders of the metal and annealed in vacuum at 900 °C. Although the dents on the surface of diamond facets were found after the thermal erosion tests, a detailed investigation of the eroded surface was not conducted. Therefore, to our best knowledge, the study reported here is the first detailed account of the crystallographic and microstructural aspects of the formation of nickel/diamond interface during sintering.

By carrying out the analysis of the microstructure formation of the volume of the material involved in sintering at the nickel/diamond interface established by bringing into

contact the particles of nickel and diamond at relatively low temperatures, we obtained evidence of interaction and suggested contact melting of a metastable eutectic as a process responsible for the interface development in this system. These results contribute to a deeper understanding of the behaviour of systems containing metastable phases and offer a pathway to explain an increased strength of materials containing nickel/diamond interfaces.

Conclusions

This study presents, for the first time, a detailed microstructural analysis of the nickel/diamond interfaces formed during sintering of powder mixtures at temperatures well below the melting point of nickel or the nickel-graphite eutectic. In the sintered compacts, the fracture of the nickel-diamond inter-particle joints was cohesive and resulted in the formation of nickel-containing patches on the diamond facets. The number of joints was greater in the Spark Plasma Sintered compact than in the conventionally sintered compact, their microstructural features remaining similar. The joints were more uniformly distributed over the surface of diamond particles in the Spark Plasma Sintered compact compared with the conventionally sintered compact. The microstructure of the patches adhered to the diamond surface, their geometry and orientation relative to the edges of the diamond crystals suggested that the formation and development of the interface involved contact melting followed by crystallization

of the melt upon cooling according to certain directions of the diamond crystalline lattice. A viable explanation of the formation of liquid at such a low temperature is contact melting of a metastable eutectic between nickel and diamond. It was shown that the composition of the gaseous atmosphere, in which sintering or annealing of nickel-diamond materials is conducted, plays a decisive role in the formation and evolution of the microstructure of the regions adjacent to the nickel/diamond interface.

Acknowledgements

This study is supported by the Russian Foundation for Basic Research, Research Project 15-33-20061 mol_a_ved.

The authors are grateful to Dr. Evgeniy N. Galashov for providing powders of synthetic diamond for the experiments, Dr. Natalia V. Bulina for her help with the X-ray diffraction analysis of the samples and Ivan N. Skovorodin for his help with hot pressing experiments.

Notes and references

- P. C. Yang, W. Zhu and J. T. Glass, *J. Mater. Res.*, 1993, **8**, 1773.
- P. C. Yang, W. Liu, R. Schlessler, C. A. Wolden, R. F. Davis, J. T. Prater and Z. Sitar, *J. Crystal Growth*, 1998, **187**, 81.
- T. Ohashi, W. Sugitomo, and Y. Takasu, *Bull. Chem. Soc. Japan*, 2011, **84**, 276.
- T. Ohashi, W. Sugitomo and Y. Takasu, *Appl. Surf. Sci.*, 2012, **258**, 8128.
- A. I. Chepurov, V. M. Sonin, A. A. Chepurov, E. I. Zhimulev, B. P. Tolochko, and V. S. Eliseev, *Inorg. Mater.*, 2011, **47**, 864.
- H. Mehedi, J.-C. Arnault, D. Eon, C. Hébert, D. Carole, F. Omnes and E. Gheeraert, *Carbon*, 2013, **59**, 448.
- H. Mehedi, C. Hébert, S. Ruffinatto, D. Eon, F. Omnes and E. Gheeraert, *Nanotechnology*, 2012, **23**, 455302.
- W. Smirnov, J. A. Hees, D. Brink, W. Müller-Sebert, A. Kriele, O. A. Williams and C. E. Nebel, *Appl. Phys. Lett.*, 2010, **97**, 073117.
- C. Artini, M. L. Muolo and A. Passerone, *J. Mater. Sci.*, 2012, **47**, 3252.
- W. Tillmann, M. Ferreira, A. Steffen, K. Rüster, J. Möller, A. Bieder, M. Paulus and M. Tolán, *Diamond&Related Mater.*, 2013, **38**, 118.
- B. Twomey, A. Breen, G. Byrne, A. Hynes and D. P. Dowling, *J. Mater. Proc. Technol.*, 2011, **211**, 1210.
- M. Singleton and P. Nash, *Alloy Phase Diagrams*, 1989, **10**, 121.
- Z. A. Munir, D. V. Quach and M. Ohyanagi, *J. Amer. Ceram. Soc.*, 2011, **94**, 1.
- M. Tokita, In: Somiya S., editor. *Handbook of Advanced Ceramics: Materials, Applications, Processing and Properties*, 2nd edition, Academic Press; 2013, p.1149.
- L.-D. Zhao, S. Hao, S.-H. Lo, C. Wu, X. Zhou, Y. Lee, H. Li, K. Biswas, T. P. Hogan, C. Uher, C. Wolverton, V. P. Dravid and M. G. Kanatzidis, *J. Am. Chem. Soc.*, 2013, **135**, 7364.
- M. Scheele, N. Oeschler, I. Veremchuk, S. Peters, A. Littig, A. Kornowski, C. Klinké and H. Weller, *ACS Nano*, 2011, **5**, 8541.
- R. Berthelot, B. Basly, S. Buffière, J. Majimel, G. Chevallier, A. Weibel, A. Veillère, L. Etienne, U. Chung, G. Goglio, M. Maglione, C. Estournès, S. Mornet and C. Elissalde, *J. Mater. Chem. C*, 2014, **2**, 683.
- A. Boden, B. Boerner, P. Kusch, I. Firkowska and S. Reich, *Nano Lett.*, 2014, **14**, 3640.
- M. Beekman, M. Baitinger, H. Borrmann, W. Schnelle, K. Meier, G. S. Nolas and Y. Grin, *JACS*, 2009, **131**, 9642.
- X. Song, X. Liu, X. and J. Zhang, *J. Am. Ceram. Soc.*, 2006, **89**, 494.
- Y. Aman, V. Garnier and E. Djurado, *J. Mater. Sci.*, 2012, **47**, 5766.
- P. Vasiliev, F. Akhtar, J. Grins, J. Mouzon, C. Andersson, J. Hedlund and L. Bergström, *Appl. Mater.&Interfaces*, 2010, **2**, 732.
- R. Marder, C. Estournès, G. Chevallier and R. Chaim, *Scripta Mater.*, 2014, **82**, 57.
- S. Rudinsky and M. Brochu, *Scripta Mater.*, 2015, **100**, 74.
- S. A. Evlashin, V. P. Martovitskii, R. A. Khmel'nitskii, A. S. Stepanov, N. V. Suetin and P. V. Pashchenko, *Tech. Phys. Lett.*, 2012, **38**, 418.
- Z. F. Guan, F. Deng, Q. Z. Liu, S. S. Lau and C. a. Hewett, *Mater. Chem. Phys.*, 1996, **46**, 230.
- B. Bokhonov and M. Korchagin, *J. Alloys Comp.*, 2002, **333**, 308.
- B. B. Bokhonov, D. V. Dudina, A. V. Ukhina, M. A. Korchagin, N. V. Bulina, V. I. Mali and A. G. Anisimov, *J. Phys. Chem. Solids*, 2015, **76**, 192.
- I. Shpilevaya, W. Smirnov, S. Hirsz, N. Yang, C. E. Nebel and J. S. Foord, *RSC Adv.*, 2014, **4**, 531.
- M. G. Nicholas, P. M. Scott and B. I. Dewar. US Patent, 4,062,660, 1977.
- T. Tanaka, N. Ikawa and H. Tsuwa, *CIRP Ann. Manuf. Technol.*, 1981, **30**, 241.